Anhydride-Cured Epoxies via Chain Reaction. 1. The Phenyl Glycidyl Ether/Phthalic Acid Anhydride System

V. Trappe and W. Burchard*

Institute of Macromolecular Chemistry, University of Freiburg, 7800 Freiburg, FRG

B. Steinmann

Plastics Division, Ciba-Geigy Ltd., 1701 Fribourg, Switzerland

Received August 13, 1990; Revised Manuscript Received March 22, 1991

ABSTRACT: The formation of linear polyesters by the anhydride-curing reaction of phenyl glycidyl ether initiated by 1-methylimidazole was studied kinetically, and the conformational properties were determined by static and dynamic light scattering and capillary viscometry. The reaction was found to follow a chain reaction mechanism, and the degree of polymerization (DP_n) obeyed the relationship $DP_n = \alpha[M_0]/[I_0]$, where $[M_0]$ and $[I_0]$ are the initial molar concentrations of monomer and initiator and α is the extent of reaction of the epoxy groups. Deviations from first-order kinetics were found and are mathematically described by initiation rate constants k_i, which are 10–50 times smaller than the propagation rate k_2. This effect is also responsible for the observed polydispersities, which are larger than for a simple Poisson process. The molecular weight dependences of the hydrodynamic radius R_h, the intrinsic viscosity $[\eta]$, and the second virial coefficient A_2 obey the scaling laws. Dimethylformamide (DMF) was chosen as solvent and found to be a typical marginal solvent. The unperturbed dimensions were determined from the Burchard–Stockmayer–Fixman and Cowie–Bywater plots for $[\eta]$ and D_z, respectively, and consistent results were obtained with the experimentally determined values of $\Phi = 2.58 \times 10^{23}$ mol^{-1} and $P_0 = 6.05$. A characteristic ratio of $C_\infty = 6.13$ and a Kuhn segment length of $l_K = 26.4 \times 10^{-8}$ cm were found for this polyester.

1. Introduction

Epoxy resins are oligomeric chemical compounds that contain one or several epoxy groups

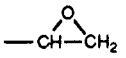

per molecule. This group has remarkable reactivity toward a number of different compounds such as amines, phenols, acids, and acid anhydrides.[1] The latter are commonly called curing agents since reactions with diepoxies or triepoxies lead to efficiently cross-linked materials with excellent physical properties. The curing process is connected with relatively small volume shrinkage.[2] Furthermore, it is a simple addition reaction, and no low molecular weight compounds are released as, for instance, in a polycondensation process.

Curing reactions have been studied extensively in the past by many investigators.[3] In most of these studies, mainly the kinetics and the mechanism of cross-linking have been the subject of interest. Also, only in rare cases has the molecular structure been investigated.[4-6] The present paper deals with both aspects.

Most curing reactions were common step reactions. In the case of acid anhydride curing, a different mechanism is effective. For the technical epoxy resins, which contain free hydroxyl groups, the curing reaction is started by the reaction of such a hydroxyl group with the anhydride, to generate a monoester with a free carboxylic acid group, and this, in turn, reacts with another anhydride:[7]

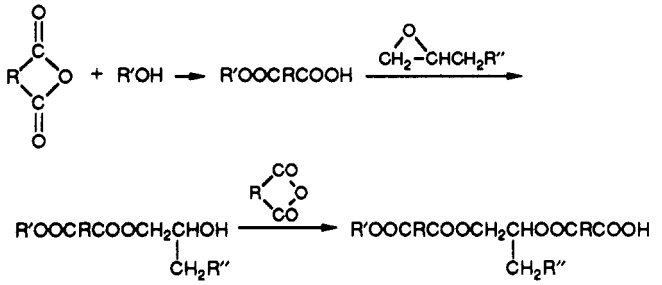

As a side reaction, ether formation by the reaction of OH groups with epoxy groups was found:[7]

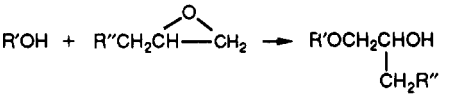

When pure, monomeric epoxides without OH groups and pure anhydrides are used, a reaction can only take place in the presence of an initiator, which can open either the epoxy ring or the anhydride.[8] The initiation by tertiary amines was studied by Matejka et al.[9] They found that the tertiary amine formed a zwitterion with the epoxide, creating a hydroxylate, which can react with anhydride:

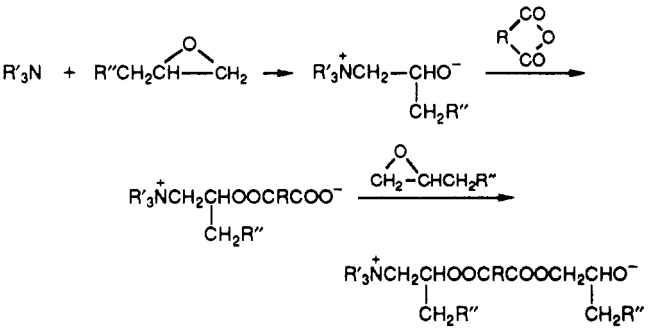

The tertiary amine seems to be irreversibly bound to the epoxide. This implies that the number of growing chains is determined by the number of initiator molecules. This mechanism represents an anionic living chain polymerization with no termination reaction. For the structure formation of the branching system, no precise predictions have been made. It is one of the main purposes of this paper to check whether such a chain reaction is indeed effective. To this end, the other requirements of a living chain reaction have to be tested. These are[10] as follows:

(1) The degree of polymerization should be determined by the molar ratio $[M_0]/[I_0]$ of monomer to initiator, where $[M_0]$ and $[I_0]$ are the initial molar concentrations of the monomer and initiator.

0024-9297/91/2224-4738$02.50/0

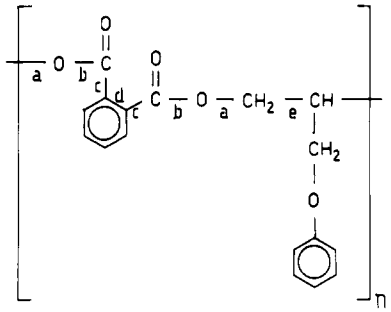

Figure 1. Repeating unit in the PGE–PA polyester. The corresponding bond lengths are a = 0.143 nm, b = 0.136 nm, c = 0.1516 nm, d = 0.1395 nm, and e = 0.1541 nm.

(2) The degree of polymerization (DP_n) should increase linearly with the extent of epoxy consumption α.

(3) The reaction should follow first-order kinetics.

(4) Very narrow molecular weight distributions should result, which under ideal conditions should obey the Poisson distribution.[11]

These four conditions can be checked, of course, only with linear chains, and for this reason, the monoepoxide phenyl glycidyl ether (PGE, 1) was chosen with phthalic acid anhydride (PA, 2) as the curing agent and 1-methylimidazole (1-MI, 3) as the initiator.

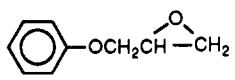

1

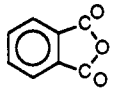

2

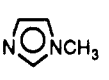

3

Matejka et al. studied, prior to us, a similar curing reaction, i.e., the copolymerization of phenyl glycidyl ether and hexahydrophthalic acid anhydride with benzyldimethylamine as the initiator.[12] This anhydride, however, undergoes side reactions that prevent the formation of high molecular weight polymers.[8] Further investigations showed that phthalic acid anhydride was a better comonomer for this reaction. High molecular weight polymers were obtained especially with 1-methylimidazole as the initiator.[13] Analysis of the polymers obtained showed a clean polyester structure. This means that side reactions, e.g., homopolymerization of the epoxide, leading to ether bonds, can be excluded for this reaction. Hence, we are dealing with a strictly alternating copolymerization and the PGE–PA compound can be considered as the repeating unit in the polyester. The chemical structure of this unit and the various bond lengths are shown in Figure 1.

The structure of the branched polymers like the polyester resulting from the reaction of diepoxides with anhydrides is often sufficiently characterized by shrinking parameters,[14] e.g., the parameter g, which is defined as the ratio[15]

$$g = \langle S^2 \rangle_b / \langle S^2 \rangle_{lin} \quad (1)$$

of the mean square radii of gyration $\langle S^2 \rangle$ of the branched (b) to the linear (lin) materials at the *same molecular weight*. Hence, a well-defined reference of linear chains is needed for a satisfactory characterization of the branched products. We applied static and dynamic light scattering and viscometry to linear chains resulting from the copolymerization of phenyl glycidyl ether with phthalic acid anhydride and determined the hydrodynamic radius $R_h = kT/(6\pi\eta_0 D_z)$, the second virial coefficient A_2, and the intrinsic viscosity $[\eta]$ in dimethylformamide (DMF). The characterization of the branched products resulting from the reaction of diepoxides with anhydrides based on the parameters determined here for the chain polymerization will be the subject of a forthcoming paper.

2. Experimental Section

Purification of the Starting Materials. PGE p.a. (Merck) was dried over CaH_2 and distilled twice at reduced pressure. PA (Merck) was recrystallized twice in toluene. To convert residual amounts of phthalic acid in phthalic acid anhydride, PA was dissolved in a 5% thionyl chloride/dioxane solution and refluxed for 2 h. After addition of cyclohexane, the precipitate was collected and recrystallized twice from toluene. 1-MI (Merck) was purified by distillation at reduced pressure.

Synthesis of the Resins. Copolymerization of PGE and PA was carried out in bulk in argon atmosphere at 80–120 °C. A well-stirred mixture of PGE and PA (1.0/1.1) was heated to the desired temperature before the addition of the initiator 1-MI. The initiator was added in pure form or dissolved in absolute toluene. This mixture was heated for 14 h. One hour after initiation, stirring was no longer possible, due to the increased viscosity of the reaction mixture. The resins obtained were clear and sometimes yellowish. These were precipitated four times in dichloroethane/ether or acetone/methanol and finally dried in vacuo at 40 °C.

Extent of Reaction. The content of epoxy groups in the epoxy resin was determined by direct potentiometric titration using a Titroprocessor E636 with a Dosimat E635 from Metrohm. The samples were dissolved in acetone to form a 1–5% solution, mixed with a tetraethylammonium bromide solution, and titrated with 0.1 N perchloric acid in acetic acid.

Refractive Index Increment. The refractive index increments were measured in DMF at 20 °C with a Brice Phoenix differential refractometer.

Light Scattering. Static and dynamic light scattering (LS) were measured simultaneously in DMF at 20 °C with an automatic goniometer and a ALV-3000 structurator/correlator from ALV-Langen, Germany. The blue line (λ_0 = 496.5 nm) of a Model 2000 argon-ion laser by Spectra Physics was used as the light source. The correlator was coupled to a Victor-Sirius PC where the data were treated on-line with the program ODL written by Eisele.[16] Details on the instrument and data evaluation are given in ref 17. The solution for LS measurements is made dust-free by filtration through Millex-HV (0.45-μm) filters and subsequently by floating the cells[18] in a swinging bucket rotor of a L5 50b Beckman ultracentrifuge at 10 000 rpm for $^1/_2$–5 h. Because of the low molecular weight of the resins, no angular dependence was detectable. Therefore, it was sufficient to measure at scattering angles from 30 to 150° in steps of 30°.

Viscometry. The viscosity of the dilute solution was measured in DMF at 20 °C in an automatic Ubbelohde viscometer by Schott, Mainz, FRG, and the intrinsic viscosity was determined from the concentration dependence as usual.

Size Exclusion Chromatography. SEC measurements were made on a HP 1090 equipped with an RI detector. Three columns (7 × 300 mm) filled with Ultrastyragel of pore sizes 1000, 500, and 100 Å were connected in series and calibrated by polystyrene standards. Tetrahydrofuran (THF) was used as solvent.

3. Kinetics and Mechanism of the Reaction

3.1. Molecular Weights. To prove the postulated chain reaction, seven samples have been synthesized to full conversion using different ratios of $[I_0]/[M_0]$. The results are listed in Table I and presented in Figure 2. The line drawn represents the theoretical prediction for a chain reaction that is[10,11]

$$M_n = M_{mon}[M_0]/[I_0] \quad (2)$$

under the assumption of instantaneous initiation. In this equation, M_{mon} is the molar mass of the repeating unit, and the quantities in square brackets denote the molar concentrations of the monomer and initiator, respectively.

In a second series, a ratio of $[I_0]/[M_0] = 10^{-2}$ was chosen and samples were taken from the reaction vessel after certain time intervals and quenched. The extent of

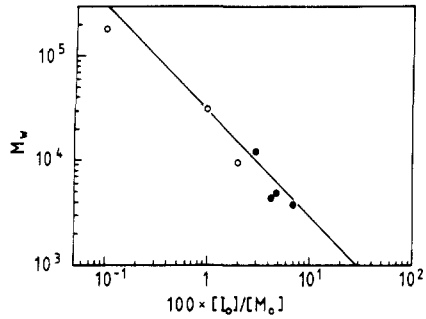

Figure 2. Change of molar masses as a function of the molar ratio of the initiator $[I_0]$ to monomer $[M_0]$ concentrations. Solid line: theoretical curve, (O) experimental values determined by light scattering, (●) experimental values determined by GPC.

Table I
Molecular Weights Measured by Static LS and by GPC as a Function of Molar Ratio of Initiator I_0 and Monomer M_0

$100[I_0]/[M_0]$	M_w(LS)	M_w(GPC)	M_w/M_n[a]
0.1	180 000		
1.0	30 000	25 300	1.22
2.0	9 600	7 800	1.31
3.0		12 300	1.34
4.3		4 300	1.62
4.8		4 800	1.39
7.0		3 700	1.36

[a] M_w/M_n denotes the polydispersity index.

Table II
Molecular Weights Measured by Static LS and by GPC and the Corresponding Polydispersity Index as a Function of the Epoxy Extent of Reaction, α ($[I_0]/[M_0] = 10^{-2}$)

α	M_w(LS)	M_w(GPC)	M_w/M_n
0.366	10 000	8 300	1.86
0.611	19 400	15 700	
0.813	25 000	21 000	1.25
0.894	27 100	20 900	1.24

reaction of epoxy was determined then by potentiometric titration according to

$$\alpha = ([E_0] - [E])/[E_0] = 1 - [E]/[E_0] \quad (3)$$

where [E] and $[E_0]$ are the epoxy concentrations at the time of reaction t and at the beginning of the reaction. Of each of these and the former samples, the molar masses were determined either by light scattering or size exclusion chromatography. The data are given in Table II. It shows the expected linear increase of M_w in the course of the monomer conversion.

The data of both series can be combined into one graph if M_w is plotted against $\alpha[M_0]/[I_0]$, Figure 3. The straight line represents the theoretical prediction for M_n.

The reaction mechanism predicts a very narrow Poisson molecular weight distribution with polydispersities of[10]

$$M_w/M_n = 1 + (M_{mon}/M_n) = 1 + [I_0]/\alpha[M_0] \quad (4)$$

in an ideal system, where M_n denotes the number-average molar mass. Values between 1.07 and 1.001 should be obtained. Much larger values were found, however (Tables I and II).

The experimental data confirm the suggested mechanism of a living chain reaction. They show, however, some scatter from the predicted values. These are probably due to the inevitable experimental errors. The synthesis is very sensitive to impurities of the starting materials, and the addition of definite, very low quantities of initiator is certainly also a source of error. Furthermore, full

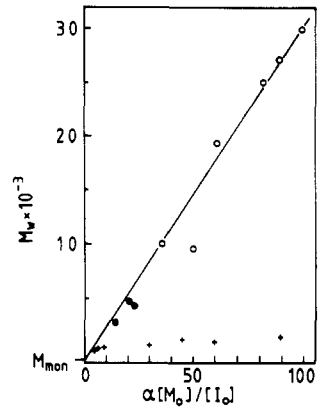

Figure 3. Plot of molar masses as a function of the extent of reaction α and the ratio of monomer to initiator. The meaning of the symbols (O, ●) and of the solid line is as in Figure 2. (+) Data obtained by Matejka et al.[12]

conversion ($\alpha = 1$) was assumed in the series shown in Figure 2. As described below, a diffusion control occurs at the end of the reaction, and full conversion may be considered to be unlikely, which explains the observed lower masses.

3.2. Kinetics. The idealized kinetic scheme is described by the following two steps

$$\sim\!\!\sim PGE^* + PA \xrightarrow{k_1} \sim\!\!\sim PA^*$$

$$\sim\!\!\sim PA^* + PGE \xrightarrow{k_2} \sim\!\!\sim PGE^*$$

with the resulting kinetic equations

$$d[PA]/dt = -k_1[\sim\!\!\sim PGE^*][PA] \quad (5a)$$

$$d[PGE]/dt = -k_2[\sim\!\!\sim PA^*][PGE] \quad (5b)$$

The time-determining step is the ring opening of the epoxy group, as the created alcoholate anion reacts virtually immediately.[12] Under such conditions, one has

$$k_1 \gg k_2 \quad (6)$$

and the two kinetic equations may be contracted into one

$$d[M]/dt = -k_2[P^*][M] \quad (7)$$

with

$$[M] \doteq [PGE\text{–}PA]$$

and $[P^*]$ is the molar concentration of growing chains.

Assuming no change of the number of chains in the course of the reaction, one has $[P^*] = [I_0]$, and eq 7 can be easily integrated, which yields

$$[M]/[M_0] = e^{-k_2[I_0]t} \quad (8)$$

or after introducing the extent of monomer (epoxy) consumption as defined in eq 3

$$1 - \alpha = e^{-k_2[I_0]t} \quad (9)$$

Thus, a plot of ln $(1 - \alpha)$ against reaction time t should yield a straight line, with a slope that gives the rate constant k_2. Three experimental runs have been made under the following conditions:

(A) The initiator was dissolved in toluene and was given in a concentration of $[I_0]/[M_0] = 2 \times 10^{-2}$.

(B) The same initiator concentration as in A was used but the initiator was added undissolved.

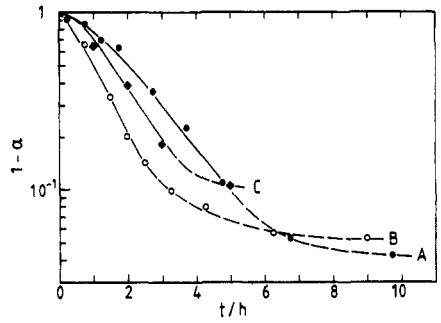

Figure 4. Plot of ln $(1 - \alpha)$ as a function of time (test for first-order kinetics). (A) $[I_0]/[M_0] = 2 \times 10^{-2}$, initiator was dissolved in toluene. (B) $[I_0]/[M_0] = 2 \times 10^{-2}$, initiator was undissolved. (C) $[I_0]/[M_0] = 1 \times 10^{-3}$, initiator was dissolved.

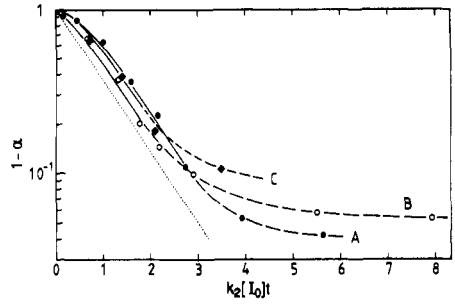

Figure 5. Same plot as in Figure 4 but now as a function of $k_2[I_0]t$. The dotted line represents the case $k_i = k_2$. The curves are shifted to the right the larger the difference $k_2 - k_i$ is.

Table III
Change of the Number of Nonreacted Epoxy Groups $(1 - \alpha)$ with Time of Reaction[a]

(A) $k_2/k_i = 27.0$		(B) $k_2/k_i = 10.2$		(C) $k_2/k_i = 45.4$	
t, h	$1 - \alpha$	t, h	$1 - \alpha$	t, h	$1 - \alpha$
0.25	0.917	0.75	0.661	1.00	0.644
0.75	0.855	1.50	0.369	2.00	0.389
1.25	0.698	2.00	0.200	3.00	0.187
1.75	0.636	2.50	0.143	5.00	0.106
2.75	0.360	3.25	0.098		
3.75	0.225	4.25	0.070		
4.75	0.109	6.25	0.057		
6.75	0.053	9.00	0.053		
9.75	0.042				

[a] (A) The initiator was dissolved in toluene; $[I_0]/[M_0] = 2 \times 10^{-2}$. (B) The initiator was undissolved; $[I_0]/[M_0] = 2 \times 10^{-2}$. (C) The initiator was dissolved in toluene; $[I_0]/[M_0] = 10^{-2}$. k_i: rate constant of initiation. k_2: rate constant of propagation.

(C) The same procedure as in B was applied but with a lower concentration ratio of $[I_0]/[M_0] = 10^{-2}$.

The results are shown in Figure 4. Only in an intermediate range of conversion is the expected linear decay observed, from which the apparent first-order kinetic rate constants k_2 were taken. The data are listed in Table III. The results of these three series of kinetic experiments can be represented in a more universal graph, if the data are plotted against the reduced time $k_2[I_0]t$, which is shown in Figure 5.

The observed behavior can be interpretated as follows. Beyond a conversion of about 85%, the curves level off, and the reaction finally completely ceases at a conversion between 90% and 98%. Such behavior is typical for the onset of a diffusion control that is caused by approaching the glass transition point, eventually having all reactions frozen in. This interpretation is supported by the fact that curve C presents the longest chain. The difference of curve A from curve B results from the fact that in run A the initiator was dissolved in toluene before injection, whereas it was added undissolved in B. Evidently the solvation of the initiator has some influence. If the rate of initiation is less than the rate of propagation, one has

$$\mathrm{I} + \mathrm{M} \xrightarrow{k_i} \mathrm{P^*}_1$$

$$\mathrm{P^*}_1 + \mathrm{M} \xrightarrow{k_2} \mathrm{P^*}_2$$

$$\mathrm{P^*}_{n-1} + \mathrm{M} \xrightarrow{k_2} \mathrm{P^*}_n \qquad (10)$$

This implies that the concentration of growing chains is not constant right from the beginning but reaches its final value only after a certain time when all initiator molecules have reacted.

Thus, instead of eq 7, a more complete kinetical scheme has to be considered

$$\mathrm{d[M]}/dt = -k_i[\mathrm{I}][\mathrm{M}] - k_2[\mathrm{P^*}][\mathrm{M}] \qquad (11)$$

Since the number of growing chains [P*] is just the number of already reacted initiator molecules, i.e., $[\mathrm{P^*}] = [I_0] - [\mathrm{I}]$, one has

$$\mathrm{d[M]}/dt = -k_2[I_0][\mathrm{M}] + (k_2 - k_i)[\mathrm{I}][\mathrm{M}] \qquad (12)$$

and

$$\mathrm{d[I]}/dt = -k_i[\mathrm{I}][\mathrm{M}] \simeq -k_i[\mathrm{I}][M_0] \qquad (13)$$

Integration yields

$$[\mathrm{I}] = [I_0] \exp(-k_i[M_0]t) \qquad (14)$$

and

$$\ln(1 - \alpha) = -k_2[I_0]t + \frac{k_2 - k_i}{k_i}\frac{[I_0]}{[M_0]}(1 - \exp(-k_i[M_0]t)) \qquad (15)$$

where the approximation was made that the monomer concentration did not change in the time interval of initiation.

The experimental curves should not be satisfactorily described with the kinetic scheme when k_i/k_2 was assumed to lie in between $^1/_{10}$ and $^1/_{50}$. The solid lines in Figures 4 and 5 correspond to this theory; the actual values are given in Table III. Equation 15 makes it clear why curves A–C do not form one common line in the plot of Figure 5. The dotted line represents the behavior when $k_i = k_2$.

The more specified kinetic system of eq 10 describes the temporal development of each growing chain $[\mathrm{P^*}_j]$ and leads to a system of coupled differential equations. This set is easily solved for $k_i \gg k_2$ by the use of generating functions and gives the familiar Poisson disribution for the chain length. When $k_i < k_2$, the integration procedure becomes rather complex. Several approaches have been published previously.[19-21] The results of our more comprehensive calculations will be reported separately in a forthcoming paper (a limit of $M_w/M_n \leq 1.4$ was derived). However, even without an analytical solution, a qualitative consideration leads immediately to the conclusion that such "creeping" initiation must cause a rather broad size distribution in the beginning of the polymerization, which should become narrower in the course of time, eventually leading to the Poisson distribution. Inspection of Table II demonstrates this behavior experimentally. Only in two cases were higher values for M_w/M_n (>1.4) found by SEC measurement, and this may be caused by traces of monomer still present in the system. These results will be checked in a further study by measurements with SEC

coupled with a low-angle laser light scattering (LALLS) detector.

4. Conformational Properties

As already mentioned in the Introduction, the determination of various conformational properties is considered to be an important task in order to gain a reliable reference state for the properties of the highly branched clusters in the corresponding diepoxy curing (e.g., Bisphenol A diglycidyl ether–phthalic acid anhydride (BADGE–PA)). Most elucidating is the determination of the shape of the particle scattering factor

$$P_z(q) = R_\Theta / R_{\Theta=0} \tag{16}$$

where

$$q = (4\pi/\lambda) \sin \Theta/2$$

with $\lambda = \lambda_0/n_0$ being the wavelength of the light in solution and n_0 being the solvent refractive index. Θ is the scattering angle, and R_Θ is the scattering intensity (Rayleigh ratio) at this angle. Most of the obtained polyesters are too small as to show deviations from unity in the series expansion of $P_z(q)$

$$P_z(q) = 1 - 1/3\langle S^2\rangle_z q^2 + \ldots \tag{17}$$

and the geometrically defined mean square radius of gyration $\langle S^2\rangle_z$ could not be measured.

The determination of the translational diffusion coefficient, D_z, however, is not restricted. Applying the Stokes–Einstein relationship as a definition, one can obtain a hydrodynamically effective radius

$$R_h = kT/6\pi\eta_0 D_z \tag{18}$$

with η_0 being the solvent viscosity.

Furthermore, the second virial coefficient A_2 and the intrinsic viscosity $[\eta]$ of the samples were measured in DMF by static LS and capillary viscometry. The results are plotted in Figures 6–8 against the molecular weight M_w on a double-logarithmic scale. The M_w dependences can be represented by

$$R_h = 1.54 \times 10^{-9} M_w^{0.53\pm0.01} \sim M^\nu, \text{ cm} \tag{19}$$

$$A_2 = 3.18 \times 10^{-2} M_w^{-0.38\pm0.05} \sim M^{a_{A_2}}, \text{ cm}^3 \text{ mol g}^{-2} \tag{20}$$

$$[\eta] = 2.8 \times 10^{-2} M_w^{0.60\pm0.05} \sim M^{a_\eta}, \text{ cm}^3 \text{ g}^{-1} \tag{21}$$

The various exponents are inter-related (scaling laws[22]), and it is indeed easy to show that in the limit of sufficiently large molecular weights

$$a_{A_2} = 3\nu - 2 \tag{22a}$$

$$a_\eta = 3\nu - 1 \tag{22b}$$

one realizes that these scaling laws for flexible chains are very well satisfied with an average value of

$$\nu = 0.53 \pm 0.01 \quad \text{PGE–PA in DMF}$$

This result may be compared with that for the linear Bisphenol A diglycidyl ether–Bisphenol A (BADGE–BA) solution in diglyme[4d,5a]

$$\nu = 0.56 \pm 0.01$$

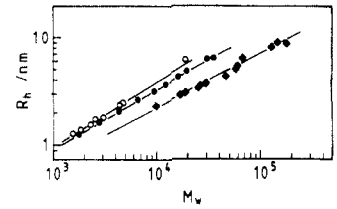

Figure 6. Molar mass dependence of the hydrodynamic radii for (●) linear BADGE–BA polyethers in diglyme, (○) strongly branched BADGE/BA polyethers in diglyme, and (◆) linear PGE–PA polyesters in DMF (this work). (BADGE = Bisphenol A diglycidyl ether, BA = Bisphenol A, PGE = phenyl glycidyl ether, PA = phthalic acid anhydride). R_h was determined from diffusion measurements using the Einstein–Stokes relationship.

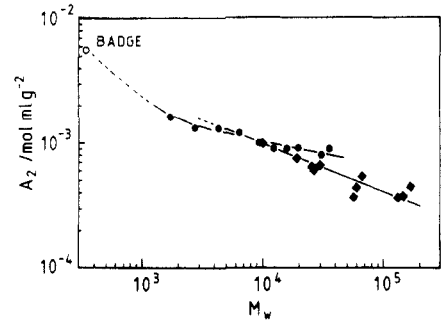

Figure 7. Molar mass dependence of the second virial coefficient for (●) linear BADGE–BA polyethers in diglyme and (◆) linear PGE–PA polyesters in DMF.

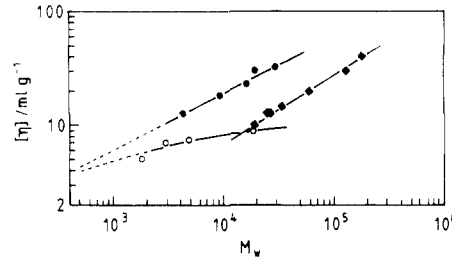

Figure 8. Molar mass dependence of the intrinsic viscosity of (●) linear BADGE–BA polyethers in diglyme, (○) strongly branched BADGE–BA polyethers in diglyme, and (◆) linear PGE–PA polyesters in DMF.

and the branched series[4d,5a]

$$\nu = 0.61 \pm 0.01$$

For comparison, the corresponding dependence of $[\eta]$ is also plotted in Figure 8. Two points are immediately obtained.

(i) The branched materials show different qualitative behavior from that of the linear chain; in particular, they no longer obey the scaling laws of eq 22. For this reason, these samples will not be discussed further in this paper.

(ii) The anhydride-cured linear polyesters show a flatter increase in the dimensions and are, in the whole range of molecular weights, considerably smaller than those of the polyethers. The exponent $\nu = 0.53$ is closer to that for a system under θ conditions ($A_2 = 0$, $\nu = 0.5$) than for a good solvent system ($A_2 > 0$, $\nu = 0.595$). Thus, DMF is for the PGE–PA polyester a typical marginal solvent. The lower absolute values would indicate a higher flexibility of the polyester compared to that of the polyether; however, see the more detailed discussion below.

This statement can be made more quantitative by applying the Burchard–Stockmayer–Fixman (BSF)[23,24] plot to the intrinsic viscosity measurements and the Cowie–Bywater (CB)[25] plot to the hydrodynamic radii (Figures 9 and 10). These plots are based on the approximate

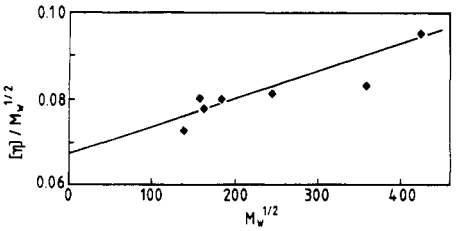

Figure 9. Burchard–Stockmayer–Fixman plot of the intrinsic viscosity data for the PGE–PA polyesters in DMF.

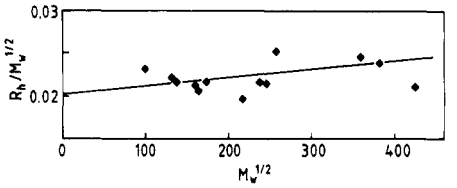

Figure 10. Cowie–Bywater plot of the hydrodynamic radii for the PGE–PA polyesters in DMF.

equations[24,26]

$$[\eta]/M^{1/2} = K_0 + BM^{1/2} \tag{23}$$

and

$$(kT/6\pi\eta_0 D)(1/M^{1/2}) = R_h/M^{1/2} = P_0 A/6\pi + B'M^{1/2} \tag{24}$$

In these equations, the constants K_0 and A are given as

$$K_0 = A^2\Phi_0 \tag{25}$$

$$A = (6R_{g,\theta}{}^2/M)^{1/2} \tag{26}$$

and contain the unperturbed dimension $R_{g,\theta}$. The two other parameters Φ_0 and P_0 are defined through the hydrodynamic interaction in viscosity and diffusion, respectively

$$\Phi_0 = 2.58 \times 10^{23}\ \text{mol}^{-1} \tag{27}$$

$$P_0 = 6.05 \tag{28}$$

Two comments have to be made here

(i) In the Fox–Flory relationship[27] for the viscosity in a Θ solvent, the theoretically predicted value[11] is $\Phi_0 = 2.84 \times 10^{23}$ mol^{-1}. The value in eq 27, however, corresponds to the experimental result of Krigbaum and Carpenter.[28,29]

(ii) The P_0 parameter contains the ratio $1/\rho = R_h/R_g$. The value $P_0 = 5.11$[11] was derived by using the Kirkwood–Riseman value for $\rho = 1.504$.[30] Experimentally, however, $\rho = 1.27$ was found in a Θ system.[31] Recently, this result has been confirmed in Monte Carlo simulations by Freire et al.[32] ($P_0 = 6.2 \pm 0.2$).

The plot in Figure 9 gives $K_0 = 0.067 \pm 0.003$ cm^3 g$^{-3/2}$ mol$^{1/2}$ and $A = (6.38 \pm 0.29) \times 10^{-9}$ cm mol$^{1/2}$ g$^{-1/2}$, and that in Figure 10 gives $AP_0/6\pi = (2.04 \pm 0.05) \times 10^{-9}$ cm mol$^{1/2}$ g$^{-1/2}$ and $A = (6.36 \pm 0.15) \times 10^{-9}$ cm mol$^{1/2}$ g$^{-1/2}$ in very good agreement to each other.

A quantitative measure of the chain stiffness is either the characteristic ratio at large M_w[33]

$$C_\infty = 6R_{g,\theta}{}^2/nl^2 \tag{29}$$

or the length of a Kuhn segment l_K,[34] which is obtained from C_∞ via[33,35]

$$l_K = lC_\infty \tag{30}$$

Both of these relationships require the knowledge of the virtual bond length l of a repeating unit ($n = M_w/M_0$ is the number of repeating units per chain, not to be mixed up with N_k, the number of Kuhn segment lengths l_K per chain). The virtual bond length can be estimated from the bond lengths of the individual bonds as given in Figure 1 and was found to be

$$l = 4.31 \times 10^{-8}\ \text{cm} \tag{31}$$

With the molecular weight of the repeating unit of $M_0 = 298.3$ g mol^{-1}, we finally find C_∞ and l_K. The values of the molecular parameters thus obtained are given in Table IV together with the results for polystyrene[36] (PS) and for the BADGE–BA linear polyether.[37] These results appear to be confusing at first sight and need detailed consideration.

Table IV
Bond Length l, Characteristic Ratio C_∞, and Kuhn Segment Length l_K for the PGE–PA Polyester, Polystyrene (PS), and the BADGE–BA Linear Polyether

	$10^8 l$, cm	C_∞	$10^8 l_K$, cm
PGE–PA	4.3	6.13	26.4
PS[36]	2.5	9.8	24.5
BADGE–BA[37]	12.8	1.34	17.2

The characteristic ratio C_∞ as introduced by Flory[33] is a measure of the extent a real chain is expanded relative to the freely jointed chain as a result of fixed bond angles and hindered rotation of the monomeric units around their bonds. Another measure for chain rigidity is the Kuhn segment length[34] l_K, which is a step length just as large as to guarantee random flight statistics. C_∞ and l_K are related to each other by eq 30. Often the Kuhn segment length is taken as a quantity that *uniquely* defines the stiffness of chains; e.g., the longer the Kuhn segment, the stiffer the chain. This view implies difficulties, because from the C_∞ data we would conclude PS to be the stiffest chain followed by a rather flexible PGE–PA (similar to polyisoprene) and finally a nearly ideally flexible BADGE–BA chain. Choosing, on the other hand, l_K as the basis, the order in rigidity would be PGE–PA > PS > BADGE–BA.

In fact, l_K is *not* a *unique* chain stiffness parameter but depends on the average bond length l of the monomeric unit. If l_K is normalized with respect to this length, the characteristic ratio is obtained. Thus, C_∞ certainly is the better parameter if chain stiffness is considered to arise from a hindered rotation. The contribution of the rodlike bond length is neglected here.

If chain stiffness is estimated from the dimensions of the coil, then the length of the bond has to be taken into account. The chain with the larger intrinsic viscosity may be expected to be the stiffer chain. Such behavior is indeed often observed, but the conclusion is not in every case correct. This can be recognized from the Fox–Flory relationship

$$[\eta] = \Phi R_g{}^3/M \tag{32}$$

which can be expressed in terms of C_∞, l, and the molar mass M_0 of the monomeric unit

$$[\eta] = (C_\infty l^2/6M_0)^{3/2} M^{1/2} \tag{33}$$

Using the data for C_∞ and l as given above and the molar masses of $M_0 = 284$ g mol^{-1} for BADGE–BA and 298 g mol^{-1} for PGE–PA, one finds for the intrinsic viscosities in the Θ state

$$[\eta]_{\text{BADGE–BA}} = 2.88[\eta]_{\text{PGE–PA}} \tag{34}$$

Although there is almost no rotational hindrance in the

BADGE–BA poly(hydroxy ether), the intrinsic viscosity and also the radii of gyration are predicted to be considerably larger than those for the PGE–PA polyester in spite of the considerably hindered rotation. The reason for this apparent contradiction arises from the much larger bond length in the poly(hydroxy ether) and contributes with its square, while C_∞ has only a linear weight (see eq 33).

Hence, if we speak of chain stiffness, we have to specify whether this quantity is based on C_∞, i.e., hindered rotation, or on the overall dimensions. As long as the bond lengths of the different polymers do not differ too much, both estimates are in line, but with strongly differing bond lengths, the opposite behavior is concluded.

Acknowledgment. We thank Dr. S. A. Zahir, Ciba-Geigy, for fruitful discussions. V.T. appreciates the opportunity of a practical course at Ciba-Geigy, Marly, Switzerland. This work was done partially within the framework of the Sonderforschungsbereich SFB 60, supported by the Deutsche Forschungsgemeinschaft.

References and Notes

(1) Neville, K.; Lee, H. *Handbook of Epoxy Resins*; McGraw-Hill: New York, 1982.
(2) Meyerhans, K. *Kunststoff Handbuch*; Vieweg: Braunschweig.
(3) Dušek, K. Epoxy Resins and Composites. *J. Adv. Polym. Sci.* **1985**, *1*, 72; **1986**, *2*, 75; **1986**, *3*, 78; **1986**, *4*, 80.
(4) (a) Burchard, W.; Bantle, S.; Zahir, S. A. *Makromol. Chem.* **1981**, *182*, 145. (b) Bantle, S.; Hässlin, W.; ter Meer, H.-U.; Schmidt, M.; Burchard, W. *Polymer* **1982**, *23*, 1989. (c) Bantle, S.; Zahir, S. A. *ACS Symp. Ser.* **1983**, *22*, 245. (d) Bantle, S.; Burchard, W. *Polymer* **1986**, *27*, 728.
(5) (a) Burchard, W.; Bantle, S.; Wachenfeld-Eisele, E. *Macromol. Chem., Macromol. Symp.* **1987**, *7*, 55. (b) Wachenfeld, E.; Burchard, W. *Polymer* **1987**, *28*, 817. (c) Wachenfeld-Eisele, E.; Burchard, W. *Polymer* **1988**, *29*, 471. (d) Wachenfeld-Eisele, E. In *Biological and Synthetic Networks*; Kramer, O., Ed.; Elsevier: London, 1988; p 305. (e) Wachenfeld-Eisele, E.; Burchard, W. *Macromolecules* **1989**, *22*, 2496.
(6) Sedladcek, B.; Kahovec, J. Crosslinked Epoxies: *Macromol. Chem., Macromol. Symp.* **1987**, *7*.
(7) (a) Fisch, W.; Hofmann, W.; Koskikallio, J. *J. Appl. Chem.* **1956**, *6*, 429. (b) Fisch, W.; Hofmann, W. *Makromol. Chem.* **1961**, *44*, 8. (c) Stevens, G. C. *J. Appl. Polym. Sci.* **1981**, *26*, 4259.
(8) Steinmann, B. *J. Appl. Polym. Sci.* **1989**, *37*, 1753.
(9) Matejka, L.; Lövy, J.; Pokorny, S.; Bonchal, K.; Dušek, K. *J. Polym. Sci., Chem. Ed.* **1983**, *21*, 2873.
(10) See textbooks on polymer science, e.g.: (a) Elias, H.-G. *Macromolecules, Synthesis and Materials*; Plenum: New York, 1977. (b) Billmeyer, F. W. *Textbook of Polymer Science*; Wiley: New York, 1984. (c) Henrici-Olivé, G.; Olivé, S. Kettenübertragung bei radikalischer Polymerisation. *Adv. Polym. Sci.* **1961**, *2*, 496. (d) Vollmert, B. *Grundriss der Makromolkularen Chemie*; E. Vollmert-Verlag: Karlsruhe, 1979; Vol. I.
(11) Flory, P. J. *Principles of Polymer Chemistry*; Cornell University Press: Ithaca, NY, 1953.
(12) Matejka, L.; Pokorny, S.; Dušek, K. *Makromol. Chem.* **1985**, *186*, 2025.
(13) Steinmann, B. *J. Appl. Polym. Sci.*, in press.
(14) Burchard, W. *Adv. Polym. Sci.* **1983**, *48*, 1.
(15) Zimm, B. H.; Stockmayer, W. H. *J. Chem. Phys.* **1949**, *17*, 1301.
(16) Eisele, M. Ph.D. Thesis, Freiburg, 1988.
(17) Bantle, S.; Schmidt, M.; Buchard, W. *Macromolecules* **1982**, *15*, 1604.
(18) Dandliker, W. B.; Kraut, J. *J. Chem. Phys.* **1955**, *78*, 2380.
(19) Gold, L. J. *J. Chem. Phys.* **1958**, *28*, 91.
(20) Nanda, V. S.; Jain, R. K. *J. Polym. Sci.* **1964**, *A2*, 4583.
(21) Dušek, K.; Somvarsky, J. *J. Polym. Bull.* **1985**, *13*, 321.
(22) de Gennes, P.-G. *Scaling Concept in Polymer Physics*; Cornell University Press: Ithaca, NY, 1979.
(23) Burchard, W. *Makromol. Chem.* **1961**, *50*, 20.
(24) Stockmayer, W. H.; Fixman, M. *J. Polym. Sci.* **1963**, *C1*, 137.
(25) Cowie, J. M. G.; Bywater, S. *Polymer* **1965**, *6*, 197.
(26) Fixman, M. *J. Chem. Phys.* **1955**, *23*, 1656.
(27) Fox, T. G.; Flory, P. J. *J. Chem. Phys.* **1949**, *53*, 197.
(28) Krigbaum, W. R.; Carpenter, D. K. *J. Chem. Phys.* **1955**, *59*, 1166.
(29) Tanford, C. *Physical Chemistry of Macromolecules*; Wiley: New York, 1961; p 401.
(30) Kirkwood, J. G.; Riseman, J. *J. Chem. Phys.* **1948**, *16*, 565.
(31) Schmidt, M.; Burchard, W. *Macromolecules* **1981**, *14*, 210.
(32) (a) Freire, J. J.; Rey, A.; Garcia de la Torre, J. *Macromolecules* **1986**, *19*, 457. (b) Rey, A.; Freire, J. J.; Garcia de la Torre, J. *Macromolecules* **1987**, *20*, 342.
(33) Flory, P. J. *Statistical Mechanics of Chain Molecules*; Wiley: New York, 1969.
(34) Kuhn, W. *Kolloid Z.* **1934**, *68*, 2.
(35) Burchard, W.; Denkinger, P. *2nd Dresden Polymer Discussion*; Akademie Verlag: Berlin, 1989; p 176.
(36) *Polymer Handbook*; Brandrup, J., Immergut, E. H., Eds.; Wiley: New York, 1975.
(37) Bantle, S. Ph.D. Thesis, Freiburg, 1982.

Registry No. 1, 122-60-1; 2, 85-44-9; 1/2 (copolymer), 30731-31-8; 1/2 (SRU), 96258-17-2.